RASĀYAN *J. Chem.*
Vol. 19 | No. 4 | 2465-2476 | October-December | 2026
ISSN: 0974-1496 | e-ISSN: 0976-0083 | CODEN: RJCABP
http://www.rasayanjournal.com
http://www.rasayanjournal.co.in

QUANTUM SIMULATION AND EXPERIMENTAL ANTIOXIDANT STUDIES OF A HALOGENATED COUMARIN DERIVATIVE WITH BIOACTIVITY PROBING

J. Sumathi[1], P. Udhayakala[1,✉], B. A. Benedict[2], and S. Savithiri[3]
[1]Department of Chemistry, Dr. M.G.R. Educational and Research Institute, Maduravoyal, Chennai-600 095,Tamil Nadu, India
[2]Department of Chemistry, Panimalar Engineering College (Autonomous), Poonamallee, Chennai-600 123, Tamil Nadu, India
[3]Department of Chemistry, Prathyusha Engineering College, Aranvoyalkuppam, Tiruvallur- 602 025,Tamil Nadu, India
✉Corresponding author: dean-che@drmgrdu.ac.in

ABSTRACT
Several naturally occurring as well as synthesised bioactive compounds, mainly used in prevalent drugs, comprise the coumarin scaffolds. These coumarin derivatives are of great importance for medicinal chemistry with substantial biological and pharmacological properties. The halogenated coumarin compound, 6-bromo-3-(2,3-dichlorophenyl carbamoyl) coumarin (6BDPCC), is analysed in this study to draw useful insights into its electronic, structural, and pharmacological properties. The physicochemical and structural characteristics of 6BDPCC are studied by spectroscopic profiling, computational quantum analysis (CQA), antioxidant activity assays (AAA), evaluation of global reactivity descriptors (GRD), and ADMET study. The characteristic peaks in the FTIR spectrum represent the existence of coumarin and carbamoyl functional groups. CQA using Density Functional Theory delivers optimised structure and thermodynamic descriptors, with a total electronic energy of −4389.805129 H, Gibbs free energy of 0.151755 H, and a dipole moment of 8.765286 D. These outcomes specify intrinsic molecular stability and a moderate net dipole moment. Investigation of the FMO energy gap of 4.24 eV indicates potential electronic transition phenomena and structural integrity. AAA discloses a concentration-based increase across all analyses. At 120 µg/mL, 6BDPCC exhibits 51.01% DPPH antioxidant performance. The FRAP analysis reveals strong reducing power and obtained 79.68% reduction. Also, the Phosphomolybdenum assay exhibited 75.36% total antioxidant capacity, indicating moderate to strong antioxidant potential depending on the assay mechanism. ADMET analysis exhibited promising ADME characteristics and high binding strength with the designated biological target. It highlights the pharmacological significance of 6BDPCC that supports future drug discovery in consistency with SDG-3(Good Health and Well-being).
Keywords: Halogenated Coumarin, FTIR, Computational Quantum Analysis, Radical Scavenging Activity, Antioxidant Assays, ADMET.
RASĀYAN *J. Chem.*, Vol. 19, No.4, 2026

INTRODUCTION

Coumarins are significant secondary metabolites that naturally exist in plants, fungi, and microorganisms.[1] The molecular formula of this coumarin is $C_{16}H_8BrCl_2NO_3$. Umbelliferone, scopoletin, and 4-hydroxycoumarin (4-HC) are generated by the catalytic action of CH_3 and hydroxyl-based oxidising at diverse positions.[2] While multifaceted coumarin derivatives obtained from the phenylpropanoid trails can be categorised into 3 types: furanocoumarins (coumarin with a furan ring), pyranocoumarins (coumarin with a pyran ring), and pyrone-substituted coumarins (basic coumarin (benzopyran-2-one) skeleton with functional moieties on the ring). Due to their special planar formations, structural tunability, extended π-conjugation, and versatile chemical reactivity, coumarin and its compounds show several biological behaviours, including antioxidant, anticoagulant, antifungal, anti-inflammatory, antimicrobial, antiviral, anticancer, and antihypertensive effects.[3] Therefore, coumarins are deemed as foundations for medicinal chemistry. For instance, they have been extensively used in the field of plant-based therapeutics.[4] Furthermore, coumarins have been used in various domains, including food

http://doi.org/10.31788/RJC.2026.1949935
This work is licensed under a CC BY 4.0 license.

additives, antioxidant reagents, sensitisers, insecticides, dyes, herbicides, cosmetics, and perfumes.[5] Recently, coumarins have been used for managing oxidative stress–related syndromes and other chronic diseases.[6] Recent research on coumarin derivatives has proved their potential to counteract free radicals through several actions, including Single Electron Transfer (SET), Hydrogen Atom Transfer (HAT), and Sequential Proton Loss Electron Transfer (SPLET).[7] These processes depend on environmental factors and molecular structure. The integration of carbonyl groups, halogen atoms, or aromatic functional moieties into the coumarin model can modify the electron dispersion, improve structural stability, and increase pharmacological activities.[8] In particular, halogenated coumarins have gained increasing interest owing to their inordinate pharmacological properties, such as enhanced bioactivity, permeability, and membrane metabolic stability.

Recently, computational chemistry combined with experimental studies has become an effective technique for analysing the electronic, topological, and biological characteristics of coumarin scaffolds. The spectroscopic profiling, CQA, and AAA afford a complete understanding of molecular structure, electronic distribution, and intermolecular interactions. For examining FMO, electron density characteristics, and GRD, we need Density Functional Theory (DFT) computations. DFT computations help reveal the molecular reactivity and chemical action.[9] The potential pharmacological properties of coumarin compounds are derived from the ADMET estimates.[10] Antioxidant capacity is an additional noteworthy property of coumarins, as oxidative stress owing to oxygen radicals plays a vital role in numerous diseases, like cancer, cardiovascular diseases, and neurodegenerative conditions.[11] Hence, evaluating the antioxidative efficiency of the coumarins through DPPH antioxidant, FRAP, and phosphomolybdenum assays can provide useful insights into their biological implications. Barman *et al.* (2025) conducted an inclusive study of coumarin derivatives through DFT computations, Hirshfeld surfaces, molecular docking, natural bond orbital predictions, ADMET profiling, and molecular dynamics studies.[12] Belbah *et al.* (2025) presented a systematic investigation of nickel–coumarin scaffolds through molecular electrostatic potentials, quantum theory of atoms in molecules studies, and non-covalent interactions.[13] This study reveals enhanced antioxidant activity and potential ADME descriptors, representing the correlation between electronic properties and pathophysiological significance. Toan *et al.* (2025) evaluated the antiproliferative activity of coumarin through DFT computations, ADMET calculations, molecular docking, and molecular dynamics analysis.[14] Luo *et al.* (2024) observed the free radical inhibition of natural coumarins through GRD. The authors calculated SET, HAT, and SPLET trails and justified antioxidant activity.[15] Bakti & Martoprawiro (2024) examined the impact of the nature and positions of functional moieties on free radical scavenging performance and pharmacokinetic appropriateness of coumarins through theoretical calculations.[16] Natural coumarins and their metal composites have been analysed to understand antioxidant behaviour, highlighting the relationship between electronic characteristics, functional moieties, and pharmacological efficacy.[17] Recent studies have examined carbamoyl-functionalized and halogenated coumarin derivatives.[18,19] These studies have shown that halogen functional moieties improve radical stabilisation, noncovalent behaviour, and electron delocalisation, whereas carbamoyl moieties increase hydrogen-bonding capacity and ADME profile. In spite of significant developments in the experimental and computational evaluation of coumarin derivatives, notable gaps persist. Current studies have focused mostly on DFT computations and ADMET analysis, with limited experimental evidence of antioxidant performance.[20,21,22.] Hence, there is a lack of comprehensive studies that combine spectral analysis, CQA, and AAA to provide valuable information about antioxidant behaviour. Besides, while antioxidant performance has been measured for diverse coumarin derivatives through theoretical calculations, the comprehensive antioxidant performance is often not described with empirical results. This research aims to analyse a halogenated coumarin compound, 6BDPCC, by integrating computational and experimental methods. The properties of the scaffold are evaluated by spectroscopic profiling, CQA, GRD, AAA, and ADMET estimates. This approach delivers a complete knowledge of the structural, electronic, and pharmacological aspects of 6BDPCC and underlines its potential implications in pharmaceutical and therapeutic research. The key contribution of this study is fourfold: This research empirically analyses the inherent properties of 6BDPCC using the FT-IR approach. The outcomes from this study demonstrate the presence of main substituents, conjugated aromatic organisations, and halogen functional moieties within the chemical

structure. The research highlights a CQA-based DFT approach to explore the electronic, structural, and pharmacological properties of 6BDPCC. By analysing GRD and reaction pathways of 6BDPCC through SET, HAT, and SPLET, the research clarifies the important free radical scavenging behaviour and demonstrates the effect of halogen and carbamoyl functional moieties of the coumarin derivative on the antioxidant potential. The theoretical studies are validated through DPPH antioxidant, FRAP, and phosphomolybdenum assays (AAA). The research assesses ADMET features to prove that 6BDPCC is non-toxic, bioavailable, and shows robust interaction energy with redox-sensitive biological targets, enhancing Sustainable Development Goal 3, supporting good health.

EXPERIMENTAL

Spectral analysis using FT-IR is conducted to prove the chemical structure, whereas FRAP, DPPH, and phosphomolybdenum analyses are employed to assess its free radical scavenging potential. A computational simulation is conducted to verify the structure through vibrational studies, followed by pharmacological interpretation.

Materials and Methods

The 6BDPCC, a coumarin derivative, is procured from Sigma-Aldrich with a purity of above 98%. The FT-IR spectrophotometer using Bruker IFS 66V with 4.0 cm^{-1} resolution is used to evaluate the molecular framework of the compound. The AAA is carried out using DPPH antioxidant, FRAP, and phosphomolybdenum assays, and the results divulge a concentration-based enhancement in antioxidant performance. For the DPPH assay, different concentrations of the compound (20-120 µg/mL) are blended with the DPPH solution and stored in a dark environment. The absorbance is tested at 517 nm to control free radical scavenging behaviour. In the FRAP analysis, the sample is treated with the FRAP blend, and the absorbance is tested at 593 nm to calculate the ferric reduction power. For the phosphomolybdenum assay, the sample is treated with a reagent containing sulfuric acid, ammonium molybdate, and sodium phosphate, stored for 30 minutes at 90 °C, and the absorbance is tested at 695 nm to estimate total antioxidant capacity. Simulation studies were accomplished through density functional theory adopting the B3LYP method using a 6-311++G(d,p) basis set for the four states: neutral compound (ArNH), radical (ArN●), anionic (ArN ●—), and cationic (ArN ●+). Swiss ADME software is used to evaluate the drug disposition and ADMET characteristics of substance 6BDPCC.

RESULTS AND DISCUSSION

The results obtained from spectroscopic analysis, CQA, AAA, GRD, and ADMET calculations deliver an in-depth knowledge of the behavioural and structural characteristics of the coumarin derivative. The experimental and theoretical analyses offer a comprehensive understanding of the structural characteristics, molecular features, and antioxidant activities of 6BDPCC. These findings support its significance for further study in pharmaceutical and therapeutic applications concerned with SDG-3.

Spectroscopic Characterization

Vibrational spectroscopy provides important data to understand the structure, electronic properties, and functional moieties of coumarin compounds. In this study, the 6BDPCC scaffold is systematically examined using an FT-IR spectrophotometer. The FT-IR spectral profile is employed to find the characteristic vibrational modes associated with the moieties C=C, N–H, C=O, and C–halogen bonds. The molecular structure and functional groups of 6BDPCC are analysed using an FT-IR spectral analyser, and the recorded spectrum is related to the vibrational modes obtained from quantum computations with the B3LYP method at the 6-311++G(d,p) level. The measured frequencies are normalised appropriately to explain nonlinear response and show strong correlation with the measured values from the spectral analyser. This reveals the dependability of the enhanced chemical structure. Table-1 shows the theoretical and observed vibrational mode identification of 6BDPCC using FT-IR. The N–H stretching vibration related to the carbamoyl group is detected in the region of ~3300 cm^{-1}, which agrees well with the calculated value. The aromatic C–H stretching dynamics appeared around 3000–3160 cm^{-1}, which indicates the existence of the coumarin and phenyl ring structures. A robust absorption band at ~1720 cm^{-1} is observed for the carbonyl vibration in the coumarin lactone ring and the amide carbonyl stretching of

the carbamoyl at ~1660 cm^{-1}. The C=C stretching modes of the aromatic rings are detected near 1580–1610 cm^{-1}, which reflects the conjugated π-electron system of the derivatives of coumarin compounds. In the 700–800 cm^{-1} region,[23] the stretching vibrations of C- Cl are observed, whereas the C–Br vibration is detected near ~ 600 cm^{-1}, in line with the halogen functional moieties on the phenyl and coumarin rings. Slight variations between experimental and computational vibrations may occur due to molecular interactions and environmental conditions in the solid state. Thus, the close agreement between the DFT-based vibrational frequencies and the experimental FT-IR spectrum confirms the structural assignment of coumarin and demonstrates the existence of main functional moieties accountable for its electronic structure and antioxidant activity. Figure-1 shows the FT-IR spectrum for 6BDPCC.

Table-1: Theoretical and Observed FT-IR Vibrational Assignments of 6BDPCCγ (Out-of-plane bending), β (In-plane bending)

Compound (6BDPCC)		
Theoretical FT-IR	Observed FT-IR	Vibration Assignment
499	504	νBr: Bond stretching mode of the C–Br bond (Br substitution).
550	555	νRing 1, 2 and 3: Framework vibration of aromatic rings (ring stability).
720	705	γ C–Cl bond (chloro-replaced aromatic compounds).
769	782	γ CH (Ring-3): aromatic C–H in ring-3 (substitution pattern).
808	823	γ Aromatic C–H bending (substitution positions on benzene rings).
887	878	γ C-H: substituted aromatic structure.
936	923	γCH (Ring-1&2): modes of C–H in rings 1 and 2.
961	964	γ C-H bending (ring substitution).
1048	1049	νC-Br: Stretching mode of C–Br bond (halogen substitution).
1085	1068	βC-H (Ring-3): aromatic C–H in ring-3.
1101	1102	βC-H: aromatic C–H bonds.
1142	1134	βC-H: (hydrogen atoms attached to aromatic system).
1185	1157	νC-H (Ring-3), γ N-H: Combination of C–H stretching and N–H bending (interaction between amide and aromatic groups).
1184	1185	νC-H (Ring-1): Aromatic C–H stretching mode in ring-1.
1391	1399	βC-C (Ring-3): In-plane bending of C–C bonds in aromatic ring-3.
1531	1531	γC-C: Skeletal mode of aromatic C–C bonds.
1564	1564	γC-C: Aromatic ring bending mode.
1579	1579	νC-C: Bond stretching mode of conjugated C–C bonds.
1603	1603	νC-C (Ring-1): Strong stretching of aromatic C–C bonds in ring-1 (conjugation).
1662	1661	νC-O: Bond stretching mode of carbonyl-associated C–O bond.
1719	1707	νC=O (Ring-2): Carbonyl bond stretching mode (existence of ketone/amide group).
3091	3065	ν_{asym} C-H: Asymmetric stretching mode of aromatic C–H bonds.
3100	3098	νC-H (ring-3): Aromatic C–H stretching mode in ring-3.
3104	3116	νC-H (ring-3): Added aromatic C–H stretching vibration.
3144	3159	νC-H (ring-3): High-frequency aromatic C–H bond stretching mode.
3308	3301	ν(N-H): Stretching mode of N–H bond (carbamoyl group)

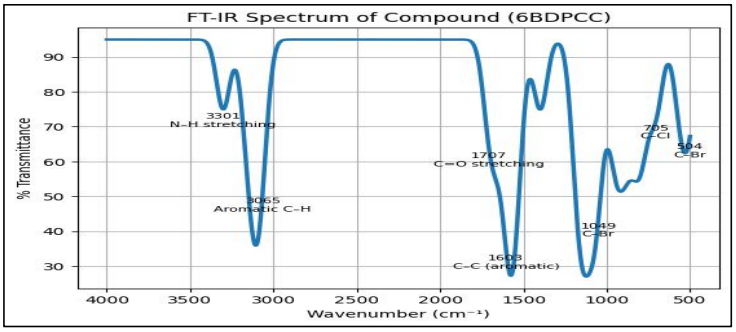


Fig.-1: FT-IR Spectrum for 6BDPCC

Computational Quantum Analysis

CQA is carried out on 6BDPCC to study its structural and electronic characteristics. The optimised molecular structure is obtained using the DFT approach; the results from these computations ensure that the improved structure is related to a stable energy minimum. Moreover, CQA offers valuable evidence about the FMO and GRD. These constraints are indispensable for understanding the electron dispersal, molecular reactivity, and internal charge transfer of the coumarin derivative.

Energy Calculations

The energy-related descriptors of 6BDPCC are computed from CQA after structural optimisation. These values deliver information about the intrinsic stability and electronic arrangement in the molecule. These parameters include the total thermal energy, electronic energy, zero-point energy (ZPE) improvement, Gibbs Free Energy (GFE), and enthalpy, which are imperative for assessing structural integrity and reactivity. The enhanced molecular structure is represented by the estimated total electronic energy of -4389.805129 Hartree. This also indicates a stable ground-state structure. The ZPE improvement (0.204212 Hartree) responsible for the vibrational motions exists even at 0 K. Thermal contributions arising from rotational, vibrational, and translational motions at 298 K produced a thermal energy of 0.223841 Hartree and a thermal enthalpy of 0.224785 Hartree. These results demonstrate that vibrational and rotational motions contribute to some extent to the total energy, increasing the stability under reference thermodynamic states. The stable thermodynamic profile with a reduced ground-state structure is represented by the GFE of 0.151755 Hartree. This value also indicates the structural integrity of the coumarin compound. The difference between the GFE and electronic energy is related to entropy-based parameters, which underlines the effect of structural variations on stability. The intended coumarin derivative has a highly polar molecular configuration with strong charge separation, which is demonstrated by the measured dipole moment (8.765286 Debye). This can increase intermolecular interactions, reactivity, capacity, and solubility. These results specify robust molecular reactions and solvent-sensitive features, which in turn influence reactivity and binding in compound systems. This confirms its interaction potential and molecular reactivity in various environments. Table-2 shows the measured energy parameters. The dipole moment parameter indicates that the 6BDPCC compound holds an intermediate polarity, which is characterised by the presence of electron-withdrawing halogen substituents (i.e., Br and Cl), carbonyl moieties, and the carbamoyl connection. This polarity enables molecular exchanges and impacts both bioactivity and molecular reactivity. The estimated values reveal that the coumarin is thermodynamically stable and demonstrates promising electronic characteristics to support its reactivity and molecular stability.

Table-2: Energy Parameters Calculated for 6BDPCC

Parameter	Value	Significance
LUMO Energy	−2.72 eV	Electron accepting ability
HOMO Energy	−6.96 eV	Electron donating ability
Energy Gap (ΔE)	4.24 eV	Molecular stability
Ionisation Potential (IP)	6.96 eV	Energy required to remove an electron
Electronegativity (χ)	4.83 eV	Tendency to attract electrons
Electron Affinity (EA)	2.72 eV	Capacity to receive electrons
Chemical Softness (S)	0.4717 eV^{-1}	Molecular polarizability
Chemical Hardness (η)	2.12 eV	Resistance to charge transfer
Chemical Potential (μ)	−4.83 eV	Overall electron escaping tendency

Electronic Properties through FMO Analysis

The electronic properties of 6BDPCC are established to underline its electron arrangements and FMO. The HOMO has an energy of −6.96 eV, primarily restricted around the nitrogen atoms and the conjugated carbon system. This indicates that the higher electron intensity regions are anticipated to participate in electron donation during molecular interactions. The LUMO lies at −2.72 eV, distributed over the aromatic rings, and reveals possible areas for electron affinity. The ΔE of 4.24 eV designates high molecular stability. The electronic density map shows limited electron density of 0.42 e/$Å^3$ around

electronegative atoms, based on the polar nature of the molecule. The electrostatic potential map reveals a range from −50 kcal/mol (most negative) to +50 kcal/mol (most positive), which highlights nucleophilic spots around nitrogen atoms and electrophilic areas over the hydrogen atoms. These results denote that the coumarin compound provides substantial electron diffusion, a higher dipole moment of 8.765286 Debye, and certain reactive areas. This makes it chemically stable and capable of participating in targeted interactions in molecular structures. Figure-2 shows that the coumarin has a stable structure with a stretched conjugated π-system. The calculated bond constraints, FMO, and energy gap divulge effective electron diffusion and charge redistribution within the molecular structure. These characteristics are vital for understanding the optical properties, molecular interactions, and potential antioxidant behaviour of the 6BDPCC compound. We investigate GRD using Koopmans' theorem to analyse the electronic features of the coumarin.[24] The electronegativity (χ) and chemical hardness (η) are estimated through the LUMO and HOMO energy parameters. The measured values of electronegativity (χ = 4.83 eV) and chemical hardness (η = 2.12 eV) denote a modest electron affinity and significant structural stability. The corresponding chemical softness (S) specifies that the coumarin compound has a certain level of polarizability. This characteristic allows reaction with oxygen-derived free radicals and contributes to its antioxidant behaviour. In addition, the electron density distribution across the molecule specifies that the core and carbamoyl group of the coumarin derivative act as important electron-dispersion centres. The presence of halogen functional moieties (Br and Cl) improves electron removal through inductive effects, which adjusts the electron dispersion and stabilises the molecular structure. These outcomes are in line with the spectroscopic fallouts and prove the electronic characteristics and structural stability of the intended coumarin compound. The measured energy gap (ΔE=4.24 eV) shows moderate structural stability and controlled charge transfer ability. The chemical hardness (η = 2.12 eV) and electronegativity (χ = 4.83 eV) indicate that the 6BDPCC retains balanced reactivity and stability. These electronic characteristics support the antioxidant performance measured in AAA and specify that the 6BDPCC can effectively participate in charge transfer processes used in oxidative stress mitigation. Table-3 shows the values of FMO energies and reactivity descriptors of 6BDPCC.

Table-3: FMO Energies and Global Reactivity Descriptors of 6BDPC

Energy Parameter	Calculated Value	Unit
Total Electronic Energy	-4389.805129	Hartree
Thermal Energy	0.223841	Hartree
ZPE	0.204212	Hartree
GFE	0.151755	Hartree
Enthalpy	0.224785	Hartree
Dipole Moment	8.765286	Debye

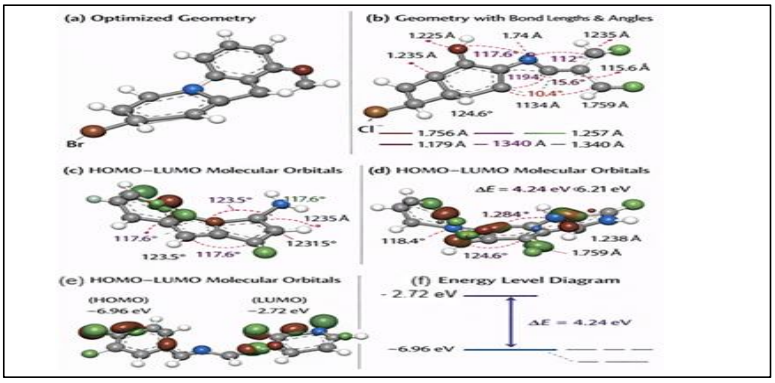


Fig.-2: Molecular Structure and Energy Level of 6BDPCC

Antioxidant Activity Assays

The antioxidant performance of the coumarin is measured using the DPPH assay, and the grades show a concentration-based increase in free radical inhibition Fig.-3. As the concentration of the molecule

increased from 20 to 120 µg/mL, the inhibition gradually increased from 7.57% to 51.01%. At lower concentrations (20 – 40 µg/mL), the compound revealed weak antioxidant activity (7.58 – 19.69%). This indicates insufficient active donor regions. A moderate increase in performance is observed at medium-level concentrations (60 – 80 µg/mL), where inhibition values reached 28.78% and 31.31%, respectively. Table-4 shows the results obtained from the AAA of the coumarin compound. A significant enhancement in scavenging performance is observed at higher concentrations (100 – 120 µg/mL), with increased inhibition values from 46.96% to 51.01%. This shows the improved free radical counteraction power of the coumarin. The gradual improvement in antioxidant activity demonstrates that the 6BDPCC shows dose-based antioxidant performance, though the maximum inhibition (~51%) indicates intermediate scavenging performance compared with strong standard antioxidants. This performance is attributed to the existence of electron-rich functional moieties, including carbonyl groups and the conjugated coumarin ring system, which allow hydrogen donation and stabilise the resulting radical species. The FRAP assay estimates the power of 6BDPCC to donate electrons and reduce Fe^{3+} to Fe^{2+}. More precisely, this assay reveals its antioxidant performance. The outcomes obtained for coumarin prove an important concentration-based increase in reducing behaviour. The absorbance increased progressively from 0.027 to 0.063 as the concentration increased from 20 to 120 µg /mL. These values represent a better reduction behaviour of ferric ions presented in Fig.-4. Also, the percentage reduction performance increased from 51.85% to 79.68% and demonstrates the robust electron-donating potential of the 6BDPCC. The 6BDPCC exhibited modest reduction capacity (51.85 – 62.85%) at lower concentrations (20 – 40 µg/mL), which denotes the early electron transfer potential of the compound. A notable enhancement is found at moderate concentrations (60–80 µg/mL), where the reduction capacity increased to 69.76% and 74.50%, correspondingly. The 6BDPCC compound provided strong reducing capacity and reached a maximum of 79.68% at higher concentrations (100–120 µg/mL). It indicates a high potential to act as a reducing agent. This remarkable reduction power is attributed to the existence of electron-rich functional moieties, including carbonyl oxygen atoms and the conjugated π-electron model of the coumarin system, which allow electron donation and stabilise oxidised species. These findings evidently advocate that the coumarin compound has substantial antioxidant performance, mostly through redox-based mechanisms. The complete free radical scavenging performance of the 6BDPCC derivative is evaluated using the phosphomolybdenum assay, which is reliant on the reduction of molybdenum ions, resulting in the growth of a green phosphate/Mo(V) complex quantifiable at 695 nm. The results demonstrate a robust concentration-related increase in antioxidant capacity, featured by a graph in Fig.-5. The absorbance values increased from 0.128 to 0.410 as the concentration increased from 20 to 120 µg/mL. These results indicate better development of the phosphomolybdenum compound. Also, the antioxidant potential increased from 21.09% to 75.36%, confirming an important improvement in reduction activity with increasing concentration. The coumarin exhibited intermediate antioxidant capacity (21.09 – 42.93%) at lower concentrations (20–40 µg/mL). A significant improvement was observed at moderate concentrations (60–80 µg/mL), where the activity increased to 58.77% and 65.05%, respectively. The coumarin derivative revealed strong antioxidant behaviour, reaching a maximum of 75.36% at higher concentrations (100 – 120 µg/mL). This shows substantial total antioxidant performance. These values indicate the donor moieties, including carbonyl regions and the conjugated model, which allow electron diffusion and stabilise the reduced Mo(V) compound. Thus, the results prove that 6BDPCC has considerable antioxidant potential, particularly using total reduction mechanisms.

Radical Scavenging Activity

In 6BDPCC, the first and second bond dissociation enthalpies of benzopyrone compounds are primarily responsible for the antioxidant action. The initial stage in the process of reactive by main antioxidants is HAT from the radical scavenging particle to the reactive transient radical species.[25,26] The radical scavenging parameters studied are represented in Table-5. The Bond Dissociation Energy (BDE) recorded as 406.28 KJ/mol^{-1} depicts a moderate antioxidant activity due to a single donor atom of Hydrogen in the N-H bond connected to the benzopyrone ring of 6BDPCC. Furthermore, the IP and Proton Dissociation Energy (PDE) parameters are evaluated by SET-PT. The computed PDE and IP

values are -414.46 KJ/mol^{-1} and 532.99 KJ/mol^{-1}, respectively. A relatively low IP value suggests a highly susceptible oxidative behaviour[27,28], and a high negative PDE value indicates the readily favourable deprotonation ability of 6BDPCC.

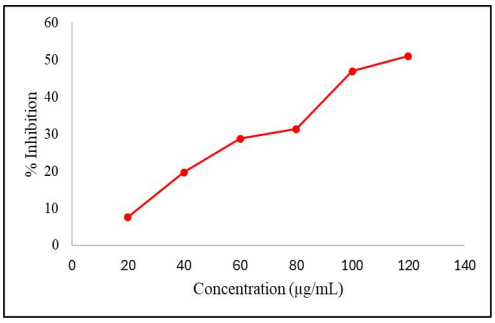


Fig.-3: DPPH Radical Scavenging Activity of 6BDPCC

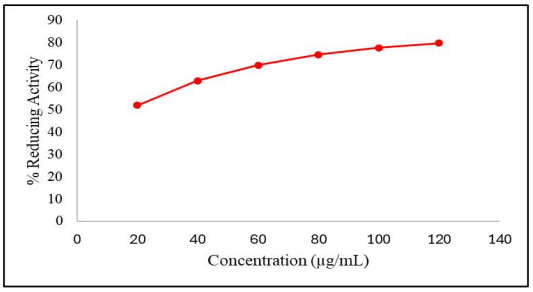


Fig.-4: FRAP of 6BDPCC

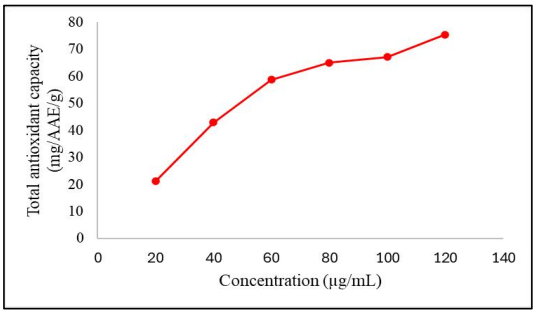


Fig.-5: Phosphomolybdenum Assay

In the solution phase, the SPLET process is prominent. The initial phase of SPLET involves proton elimination from the compound.[29,30] The generated anion's proton affinity (PA) is commonly used to represent the reaction enthalpy. Electron Transfer Enthalpy (ETE) acts as the reaction enthalpy for the next stage of the SPLET process. The observed PA (22.45 KJ/mol^{-1}) and ETE (96.07 KJ/ mol^{-1}) values indicate the interaction of 6BDPCC with radicals that have desirable reduction potentials. It is proposed that 6BDPCC could act as an electron-based antioxidant in solution. It is evident from the investigations that 6BDPCC will be a strong coumarin compound for radical scavenging activity because electron-withdrawing substituents (Br, Cl) may modulate electron density. The effect of substituents in the benzopyrone ring is insignificant for the biological activity.[31,32] In addition to radical scavenging ability, the N-H group in 6BDPCC prominently binds to enzymes that regulate oxidative stress.

Table-4: Antioxidant Activity Results of 6BDPCC

Assay Method	Concentration (µg/mL)	Absorbance	% Inhibition /% reducing activity
DPPH Radical Scavenging	Control	0.198	-
	20	0.183	7.58
	40	0.159	19.69

	60	0.148	28.78
	80	0.136	31.31
	100	0.106	46.96
	120	0.096	51.01
FRAP Assay	Control	0.013	-
	20	0.027	51.85
	40	0.035	62.85
	60	0.042	69.76
	80	0.051	74.5
	100	0.058	77.58
	120	0.063	79.68
Phosphomolybdenum Assay	Control	0.101	-
	20	0.128	21.09
	40	0.177	42.93
	60	0.245	58.77
	80	0.289	65.05
	100	0.307	67.1
	120	0.41	75.36

Table-5: Anti-oxidant Reactive Descriptors of Compound – 6BDPCC

Anti-oxidant reactive descriptors	Compound – 6BDPCC
BDE	406.28
IP	532.99
PDE	-414.46
PA	22.45
ETE	96.07

ADME Analysis

The examination of critical factors, such as the number of Hydrogen Bond Acceptors (HBA), Hydrogen Bond Donors (HBD), Topological Polar Surface Area (TPSA), rotatable bonds, water solubility, Blood-Brain Barrier (BBB) permeability, and Lipinski's Rule of Five (LRF) violations, 33 are summarised in Table-6. The results of this study of HBD and HBA for any medication molecule should always be less than 10, and in this study, 6BDPCC records the same with HBD 3, HBA 1, indicating that 6BDPCC is a good drug, as presented in Table-6. 6BDPCC demonstrated effective drug transport across biological barriers, with TPSA values of 59.31 Å2. The compound is found to have a partition coefficient (Log P) of less than five, indicating strong permeability across cell membranes. With very minor variances, the substances satisfied LRF, showing their capacity for oral bioavailability. The aqueous solubility (Log S) of 6BDPCC is computed to be -5.8 (ESOL scale), ranging from soluble to moderately soluble. The investigated drug has high GI absorption and is BBB permeant. The 6BDPCC have a bioavailability score of 0.55, indicating permeability (the rate at which a medication may pass through biological membranes) and bioavailability (the drug's ability to be absorbed or used by the body). ADME analysis specifies that the coumarin has outstanding pharmacokinetic characteristics and is widely used as a potential therapeutic candidate. The cytochrome enzymes in the liver and other tissues account for oxidative metabolic processes. CYP enzymes (CYP3A4, CYP1A2, CYP2C9, CYP2C19, and CYP2D6) cooperatively arbitrate the metabolic processes of medicines, which highlights their position in pharmacology and therapeutic studies. The CYPs' collaboration with 6BDPCC demonstrates the robust relations between 6BDPCC and CYP1A2, CYP2C19, and CYP2C9 inhibitors, but it does expose an attraction towards CYP2D6 and CYP3A4 inhibitors. The logKp value (−5. 34 cm/s) of 6BDPCC indicates dermal permeability, which indicates the lower-level infiltration of 6BDPCC through the skin, which is common for medicines recommended for oral use. The 6BDPCC effectively passed through the PAINS (Pan-Assay Interference Compounds) testing without any cautions (0 alerts), which indicates that it does not participate in false-positive signal generation and does not lead to assay interference effects. The synthetic

score of 2.76 (on a scale of 1, denoting very easy and 10 denoting very hard) denotes that 6BDPCC can be produced with relative ease. This makes it available for laboratory manufacturing and improvement.

Table-6: ADMET Characteristics of 6BDPCC

Physicochemical Properties	Value	Lipophilicity Profile (Log P_o/w)	Value	Water Solubility	Value
Formula	$C_{16}H_8BrCl_2NO_3$	iLOGP	2.91	ESOL (Log S)	-5.8
Molecular weight	413.05 g / mol	XLOGP3	4.9	Solubility	6.48e-04 mg / mL; 1.57e-06 mol / L
Number of heavy atoms	23	WLOGP	4.92	Class	Moderately soluble
Number of aromatic heavy atoms	16	MLOGP	4.11	Ali (Log S)	-5.88
Fraction Csp^3	0	SILICOS-IT	5.03	Solubility	5.43e-04 mg / L; 1.31e-06 mol / L
Number of H-bond donors	1	Consensus	4.37	Class	Moderately soluble
Number of H-bond acceptors	3			SILICOS-IT (Log S)	-8.12
Number of rotatable bonds	3			Solubility	3.11e-06 mg / mL; 7.53e-09 mol / L
Molar Refractivity	94.42			Class	Poorly soluble
TPSA	59.31 $Å^2$				
Pharmacokinetics		Drug likeness Evaluation		Medicinal Chemistry	
GI absorption	High	Lipinski	Yes (0 violation)	PAINS alert	0
P-gp substrate	No	Ghose	Yes	Brenk alert	1 (Coumarin-like moiety)
BBB permeant	Yes	Muegge	Yes	Synthetic accessibility	2.76
CYP1A2 inhibitor	Yes	Egan	Yes		
CYP3A4 inhibitor	No	Veber	Yes		
CYP2C9 inhibitor	Yes	Lead-likeness	No (MW > 350, XLOGP3 > 3.5)		
CYP2C19 inhibitor	Yes	Bioavailability Score	0.55		
CYP2D6 inhibitor	No				
Log Kp (skin permeation)	-5.34 cm/s				

CONCLUSION

This research aims to analyse the electronic, structural, and biofunctional characteristics of the halogenated 6BDPCC using spectroscopic characterisation, CQA, antioxidant studies, and ADMET predictions. The results gained from the FT-IR study demonstrate the effective formation of the molecule and confirm the presence of representative functional moieties, including carbonyl, amide, aromatic, and halogen functional moieties within the coumarin structure. The CQA provides a significant understanding of the molecular structure, energy descriptors, and electronic configuration of the coumarin. The measured ΔE indicates good chemical stability and chemical reactivity. Moreover, the GRD reveals the electron-accepting and donating abilities of the molecule. AAAs demonstrate that 6BDPCC shows

concentration-based free antioxidant and reducing potentials, as demonstrated by the DPPH, FRAP, and phosphomolybdenum assays. Additionally, the ADMET predictions indicate promising drug disposition features and potential biological interactions with target proteins, promoting the aim of SDG-3. The empirical and computational results deliver a complete understanding of 6BDPCC and prove that this coumarin may act as a potential candidate for further medicinal and pharmaceutical chemistry research. Future studies emphasise the exploration of the therapeutic potential of 6BDPCC, such as anti-inflammatory, antimicrobial, and anticancer assays, to validate its projected bioactivity.

ACKNOWLEDGMENTS

Authors are thankful to the authorities of their institutions.

CONFLICT OF INTERESTS

The authors declare that there is no conflict of interest.

AUTHOR CONTRIBUTIONS

The present work is related to *SDG-3: Good Health and Well-being*. All the authors contributed significantly to this manuscript, participated in reviewing/editing and approved the final draft for publication. The research profile of the authors can be verified from their ORCID ids, given below:

J. Sumathi https://orcid.org/0000-0001-7126-3244
P. Udhayakala https://orcid.org/0000-0002-2206-7295
B. Anna Benedict https://orcid.org/0000-0002-8470-1634
S. Savithiri https://orcid.org/0000-0002-4715-7203

Open Access: This article is distributed under the terms of the Creative Commons Attribution 4.0 International License (http://creativecommons.org/licenses/by/4.0/), which permits unrestricted use, distribution, and reproduction in any medium, provided you give appropriate credit to the original author(s) and the source, provide a link to the Creative Commons license, and indicate if changes were made.
Cite this article as: J. Sumathi *et al.*, *Rasayan J. Chem.*, 19(4), 2465-2476(2026), https://doi.org/10.31788/RJC.2026.1949935

REFERENCES

1. Y. Zou, Y. Teng, J. Li, Y. Yan, *Green Chemical Engineering*, **1**, 150(2024), https://doi.org/10.1016/j.gce.2023.04.003
2. A. Lacy, R. O'Kennedy, *Current Pharmaceutical Design*,**10**, 3797(2004), https://doi.org/10.2174/1381612043382693
3. D. Chaudhary, P. Bedi, S. Santra, T. Pramanik, *Letters in Organic Chemistry*, **19**,362(2022), https://doi.org/10.2174/1570178618666210202152452
4. A. Citarella, S. Vittorio, C. Dank, and I. Ielo, *Frontiers in Chemistry*, **12**, 1362992(2024), https://doi.org/10.3389/fchem.2024.13629922
5. M. Samanth, M. Bhat, *Russian Journal of Bioorganic Chemistry,* **50**, 1672(2024), https://doi.org/10.1134/S1068162024050108
6. Y. F. Mustafa, *Phytomedicine Plus*, **5**, 100857(2025), https://doi.org/10.1016/j.phyplu.2025.100857
7. M. Yildirim, S. Poyraz, M. Ersatir, *Medicinal Chemistry Research,* **32**, 617(2023), https://doi.org/10.1007/s00044-023-03025-x
8. M. M. Popa, D.G. Dumitrescu, S. Shova, I. Man, A. van der Lee, F. Dumitrascu, *Journal of Molecular Structure,* **1292**, 136112(2023), https://doi.org/10.1016/j.molstruc.2023.136112
9. A.K. Sharma, G.R. Nishad, P.K. Vishwakarma, P.S. Jaget, *In Computational Modelling and Simulations for Designing of Corrosion Inhibitors*, 115(2023), Elsevier, https://doi.org/10.1016/B978-0-323-95161-6.00001-1
10. M.I. Hussain, Q.A. Syed, M.N.K. Khattak, *Biologia*, **74**, 863(2019), https://doi.org/10.2478/s11756-019-00242-x
11. L. Todorov, L. Saso, I. Kostova, *Pharmaceuticals*, **16**, 651(2023), https://doi.org/10.3390/ph16050651

12. R. Barman, B. Ahmed, H. Deka, P. Barukial, D. Baishya, B. Bezbaruah, *Indian Journal of Biochemistry and Biophysics*, **62**, 827(2025), https://doi.org/10.56042/ijbb.v62i8.16568
13. H. Belbah, K. Belguidoum, Z. Ourdjini, F.Z. Hamamdia, F. Madi, L. Nouar, M. Nacef, M.H. Belhachemi, H. Amira-Guebailia, A. Chouaih, *RSC Advances*, **15**, 30102(2025), https://doi.org/10.1039/D5RA03168K
14. D. N. Toan, D.T. Van, N.D. Thanh, *New Journal of Chemistry*, **49**, 16397(2025), https://doi.org/10.1039/D4NJ05437G
15. L. Luo, P. Xia, D. Zeng, *Frontiers in Science and Engineering,* **4**, 132(2024), https://doi.org/10.54691/a84b5r30
16. A.B. Bakti, M.A. Martoprawiro, *Walisongo Journal of Chemistry,* **7**,181(2024), https://doi.org/10.21580/wjc.v7i2.23327
17. L. Todorov, L. Saso, I. Kostova, *Pharmaceuticals*, **16**, 651(2023), https://doi.org/10.3390/ph16050651
18. B. Halliwell, J.M.C. Gutteridge, Free radicals in biology and medicine, 5th ed.; Oxford University Press, Oxford, 2015, https://doi.org/10.1093/acprof:oso/9780198717478.001.0001
19. P. Politzer, J.S. Murray, T. Clark, *Physical Chemistry Chemical Physics* **12**, 7748(2010), https://doi.org/10.1039/C004189K
20. R. Palabindela, R. Bodapati, P. Myadaraveni, G. Ramesh, M. Kasula, *Journal of Molecular Structure*, **1317**, 139067(2024), https://doi.org/10.1016/j.molstruc.2024.139067
21. M. Guerfi, M. Berredjem, A. Dekir, A, *Molecular Diversity* **28**, 1023(2024), https://doi.org/10.1007/s11030-023-10630-w
22. N. Flores-Holguín, J. Frau, D. Glossman-Mitnik, *ChemistryOpen*, **10**, 1142(2021), https://doi.org/10.1002/open.202100178
23. N. Karthikeyan, J. Joseph Prince, S.Ramalingam, S.Periandy, *Spectrochimica Acta, Part A: Molecular and Biomolecular Spectroscopy,* **124**, 165(2014), https://doi.org/10.1016/j.saa.2013.12.105
24. J. Frau, F. Munoz, D. Glossman-Mitnik, *Chemical Informatics*, **2**, 7(2016), https://doi.org/10.21767/2470-6973.100021
25. S.M. Shakir and Y.K. Al-Majedy, *Journal of Applied Sciences and Nanotechnology,* **2**, 20(2022), https://doi.org/10.53293/jasn.2021.4164.1076
26. J. Rimarčík, V. Lukeš, E. Klein and M. Ilčin, *Journal of Molecular Structure THEOCHEM*, **952**, 25(2010), https://doi.org/10.1016/j.theochem.2010.04.002
27. J. Chen, J. Yang, L. Ma, J. Li, N. Shahzad and C.K. Kim, *Scientific Reports*, **10**, 2611(2020), https://doi.org/10.1038/s41598-020-59451-z
28. D.M. Simijonović, D.A. Milenković, E.H. Avdović, Z.B. Milanović, M.R. Antonijević, A.D. Amić, Z. Dolićanin and Z.S. Marković, *Antioxidants*, **12**, 1858(2023), https://doi.org/10.3390/antiox12101858
29. H. Zhou, X. Li, Y. Shang and K. Chen, *Antioxidants*, **8**, 590(2019), https://doi.org/10.3390/antiox8120590
30. L. Balewski, S. Szulta, A. Jalińska and A. Kornicka, *Frontiers in Chemistry*, **9**, 781779(2021), https://doi.org/10.3389/fchem.2021.781779
31. W. Horton and M. Török, *Green Chemistry*, **Chapter 3.7**, 963(2018), https://doi.org/10.1016/B978-0-12-809270-5.00032-7
32. M.B. Majnooni, S. Fakhri, A. Smeriglio, D. Trombetta, C.R. Croley, P. Bhattacharyya, E. Sobarzo-Sánchez, M.H. Farzaei and A. Bishayee, *Molecules*, **24**, 4278(2019), https://doi.org/10.3390/molecules24234278
33. C.A. Lipinski, *Drug Discovery Today: Technologies*, **1**, 337(2004), https://doi.org/10.1016/j.ddtec.2004.11.007

[RJC-9935/2026]